A Theoretical Investigation on the Dual-Mode Photoswitching Mechanism of Some Chiroptical Systems

S. F. Braga and D. S. Galvão*

Instituto de Física, Universidade Estadual de Campinas - UNICAMP, Campinas, São Paulo, Brazil, CEP 13083-970, CP 6165

P. M. V. B. Barone and S. O. Dantas

Departamento de Física, Universidade Federal de Juiz de Fora - UFJF, Juiz de Fora, Minas Gerais, Brazil, CEP 36036−330

Received: March 30, 2001; In Final Form: June 17, 2001

The synthesis of dual-mode optical molecular switching systems has been recently achieved. These systems were based on chiral helical-shaped alkenes in which the chirality can be reversibly modulated by light. In this work we report a theoretical study on the geometric and spectroscopic properties of these structures using the well-known semiempirical methods PM3 (parametric method 3) and ZINDO/S-CI (Zerner's intermediate neglect of differential overlap/spectroscopic-configuration interaction). Our results show that there are two stable conformers very close in energy for each possible molecular helicity presenting a barrier of ∼40 kcal/mol for bond rotation along the main molecular axis. Under protonation these barriers increase significantly and might explain why the protonation leads to the blocking of the switching process. We propose a scheme for the switching mechanism based on charge transfer and conformational changes during the isomer interconversion.

1. Introduction

There is a great interest in molecular switching processes in part due to the possibility of optical information storage at the molecular level.[1] The design of functional devices at the molecular level has been the object of intense theoretical and experimental research in the past years.[2−12] Among these systems, photochemically switchable bistable organic molecules have a special appeal due to their possible technological applications in reversible optical data storage and optical computing.

However, to be of practical application there are some requirements that those molecules need to fulfill:[7,10] (a) thermal isomeric stability; (b) possibility of many repeatable cycles (read and write processes, for instance) without loss of activity; (c) ready detectability of two different isomers; (d) retention of all these properties when the molecular structures are integrated into macromolecular systems.

The bistability requirement is very fundamental and it might be based on various molecular properties such as electron transfer, isomerizations, and photocyclizations, whereas light, heat, chemical reactions, magnetic and electric fields, etc. trigger the process. Progress along these lines in order to obtain feasible systems has been made in the past years,[1−3] in particular by Feringa and collaborators.[4−10]

Feringa et al.[6,8,9] have reported the synthesis of dual mode optical molecular switching based on chiral helical-shaped alkenes in which chirality, fluorescence, and UV/VIS spectra can be reversibly modulated by light (Figure 1). More recently,[7] the same group has reported the photoresolution of the bistable compound as a dopant in a nematic liquid crystalline phase by circularly polarized light. Therefore, the chiral information of light is transmitted to the bistable molecule, followed by amplification and macroscopic expression of chirality. These important results clearly indicate the feasibility of chiral systems for optical storage and/or optical computing.

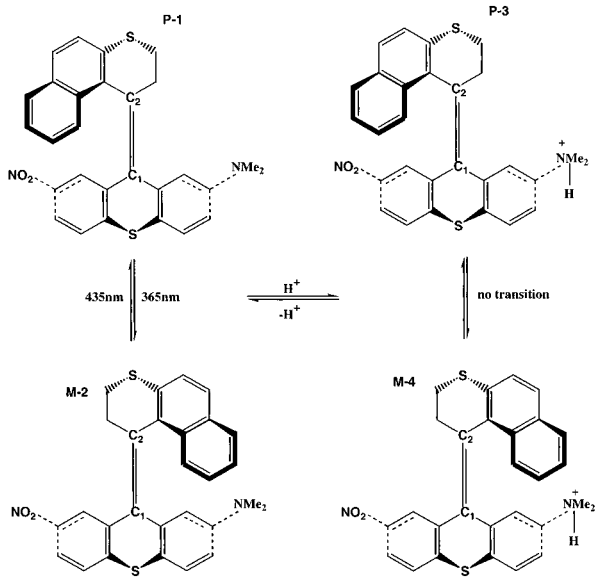

Figure 1. Molecular structures for cis (**P-1**), trans (**M-2**), and their protonated forms (**P-3** and **M-4**). See text for their descriptive names. Scheme adapted from ref 9.

The molecular system indicated in Figure 1[9] is based on donor−acceptor substituted inherently nonsymmetric thioxanthene derivatives. Photoisomerization from cis-nitro to trans-

* Corresponding author: galvao@ifi.unicamp.br, FAX: 55-19-3788-5376.

10.1021/jp011220h CCC: $20.00
Published on Web 08/07/2001

nitro, and vice-versa, can be detected by chiroptical techniques. Reversible protonation in the dimethylamino group can regulate the switching process. Due to these remarkable properties these compounds are very promising building blocks for optical memory devices as well as model systems for theoretical investigations on those aspects.

In this work we have theoretically investigated the compounds and processes indicated in Figure 1. In particular, we have analyzed aspects such as molecular stability, ground and excited-state properties, chirality, cis−trans isomerization, charge transfer, and electronic absorption spectra. The main goals of this work are to explain the mechanisms related to the cis−trans interconversions of neutral isomers as well as to elucidate the reasons of the switching inhibition when protonation takes place.

2. Methodology

Because geometric experimental data for all the structures shown in Figure 1 are not available, systematic geometric optimizations are required. The size of the structures and the need to carry out detailed conformational and chiral analysis preclude the use of good quality ab initio methods. However, these calculations are feasible in the framework of semiempirical methods. Sophisticated semiempirical methods such as MNDO[13] (modified neglect of differential overlap), AM1[14] (Austin method 1), and PM3[15] (parametric method 3) provide a good balance between quality and computational effort, and they have been successfully used to treat organic compounds.[16]

The AM1 method has been developed in an attempt to correct some of the MNDO weaknesses. In AM1, as in MNDO, the two-center nuclear attraction integrals are retained, but the MNDO tendency to overestimate the repulsion between atoms is corrected by a suitable modification of the core repulsion function.[14] PM3 has been introduced as a new formulation of these methods in order to improve MNDO and AM1 results. Basically PM3 maintains the same AM1 Hamiltonian but with a new set of parameters. However, although it is usually agreed that AM1 is better than MNDO, there is an ongoing debate[17−20] about the relative merits of AM1 and PM3.

For the structures shown in Figure 1, structural X-ray data have been published only for P-1.[8] We have used these data as a case study to compare AM1 and PM3. PM3 produced better results (see section 3) and was our choice to carry out the geometric optimizations.

Geometric and electronic features such as bond-lengths, bond-angles, dihedrals, heats of formation, dipole moment values, etc. are well described by PM3, but the electronic transitions are overestimated, as expected from a zero differential overlap (ZDO) method without configuration interaction (CI) corrections. Thus, to obtain a more realistic description of the electronic transitions, i.e., to simulate the absorption spectra, it is necessary to use methods specially developed to handle these aspects. We have chosen the ZINDO/S-CI (Zerner's intermediate neglect of differential overlap/spectroscopic-configuration interaction) method in a version specially calibrated to study organic compounds.[21−22] We have carried out ZINDO/S-CI calculations using on average 200 configurations (singlet/triplet) with the geometries obtained from PM3 calculations. We have used the Mataga−Nishimoto approach for the gamma integrals with the usual interaction factors[22] of 1.267 and 0.585. The ZINDO average errors are of only 1000−2000 cm^{-1} (∼0.1−0.2 eV) for all bands below 45000 cm^{-1}.[16] This methodology (PM3 geometries for ZINDO/S calculations) has been previously used with success in the description of organic molecules.[19,20,23,24] The simulated absorption spectra are generated by Lorentzian enveloping (half-width of 0.05 eV) the ZINDO transition energies weighted by the oscillator strength values.

3. Results and Discussions

In Figure 1 we schematically show the dual-mode optical molecular switching system based on chiral helical-shaped alkenes in which chirality and fluorescence can be reversibly modulated by light.[9] The chiroptical molecular switch is based on donor−acceptor substituted inherently dissymmetric alkenes *cis*- and *trans*-2-nitro-7-(dimethylamino)-9-(2′,3′,-di-hydro-1′-H-naphtho [2,1-b]thiopyran-1′-ylidene)-9H-thioxanthene (**P-1** and **M-2**, respectively). Under appropriate irradiation, a highly stereoselective reversible photochemical isomerization takes place [**P-1** (cis-nitro) to **M-2** (trans-nitro), and vice-versa]. This selectivity is attributed to the interaction of the upper naphthalene moiety, located either opposite the dimethylamino arene donor unit or the nitro arene acceptor unit of the lower thioxanthene part of these molecules.[9]

The switching process can be blocked by protonation of the dimethylamino donor unit. The effectiveness of the donor−acceptor system is then lost owing to a noneffective acceptor−acceptor unit in the bistable chiral alkenes. After deprotonation, the photochemical switching process between **P** and **M**-helices (**P-1** to **M-2**) is fully restored.[9] The system works as a switchable molecular device with distinct states. These states have a photon-dependent photomodulation that can be used to store information through EDRAW (erasable direct read after write) process.[9]

The objectives of the present work are (a) to theoretically characterize these distinct states and (b) to theoretically investigate why protonation blocks the switching process.

As mentioned in the methodology section, there is an ongoing debate[17−20] about the relative merits of AM1 and PM3. We have started comparing AM1 and PM3 geometrical results to the experimental X-ray data[8] for the only available structure (**P-1**, see Figure 1) in order to choose the best method. The results for the most relevant bond-lengths, bond-angles and dihedrals are available as Supporting Information. The PM3 method has clearly produced better results than AM1, thus PM3 was our choice in the geometric calculations. The PM3 results are in excellent agreement with the experimental X-ray data, considering that the theoretical data are for isolated molecules (gaseous phase) and the experimental data are for condensed-phase molecules.

We have analyzed ground and excited states (geometries, heats of formation, and conformational searches) for the four distinct structures shown in Figure 1 (**P-1**, **M-2**, **P-3**, and **M-4**). The switching process is related to an asymmetrical reversible cis/trans conformational transition coupled to a chirality inversion. This process is very complex and involves simultaneous changes in many important dihedral angles associated with chiral inversions. The determination of the structural changes involved in a **P** to **M** transition is very difficult, and even the use of the linear synchronous transit method[25] for the transition search failed. However, we can obtain an estimate for barrier interconversion from **P** to **M** structures calculating the rotational barrier about the C_1-C_2 bond and comparing the differences for the heats of formation at critical angles for ground and excited states.

In Figure 2 we show rotational barrier results for all the four structures shown in Figure 1. For the ground states, the barriers have been calculated starting from **P** or **M** configurations and performing a 180° rotation around C_1-C_2 double bond in steps of 5 degrees, keeping the chirality unaltered. For each fixed

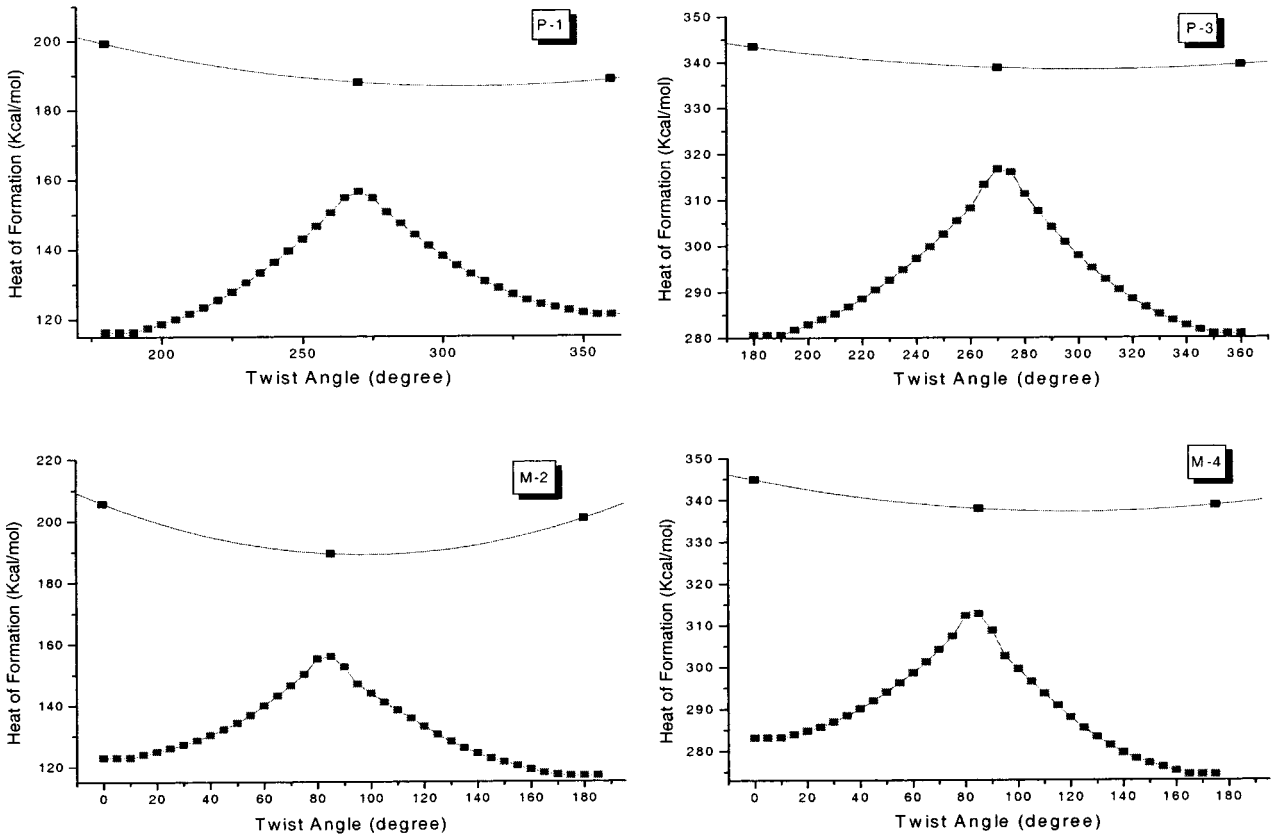

Figure 2. Ground (lower curve) and first excited singlet state (upper curve) rotational barrier curves for the four structures shown in Figure 1. The reference angle is defined by the atoms 12, 4, 9′, and 9a′ (see Supporting Information).

TABLE 1: PM3 Summary Results for the Ground, First Excited States, and Rotation Barrier around C_1-C_2 Bond, Labeled According to Figure 1[a]

molecule	A (kcal/mol)	A′ (kcal/mol)	(A to A′) (eV)	B (kcal/mol)	B′ (kcal/mol)	(B to B′) (eV)	HB (eV)	C (kcal/mol)	C′ (kcal/mol)	(C to C′) (eV)	SE (kcal/mol)
P-1	115.14	199.25	3.65	120.44	188.56	**2.96**	1.84	157.52	187.86	1.32	11.39
M-2	116.94	200.53	**3.63**	121.45	205.61	3.65	1.79	158.51	189.24	1.33	11.29
P-3	279.43	343.40	2.78	279.50	339.30	2.59	1.70	318.69	338.70	0.87	4.70
M-4	273.58	344.87	3.09	281.81	338.66	2.47	1.82	315.50	337.87	0.97	7.00

[a] The heats of formation for the ground (A,B), excited states (A′,B′), and the intermediate points (C,C′) are displayed. The differences for the vertical transitions (X to X′), the height of barrier (HB), and the stabilization energy [C′ to A′ or C′ to B′](SE) are also indicated. Due to the asymmetric character of the rotation barrier (A→C or B→C, in Figure 3), the displayed HB values are for the highest ones. The boldface entries indicate the values for the isomerization interconversion P-1→M-2.

angle we have carried out fully geometrical optimizations. Due to the high computational cost (~100 hours of CPU time in a Pentium II 400 MHz with 256 MB of RAM memory) only the necessary critical points (0, 90, and 180 degrees) have been calculated for the excited states. The PM3 conformational search has been carried out using the Chem2Pac[26,27] program package.

As we can see from Figure 2, the form of the curves is similar, differing only at the relative values for barrier height and vertical excitation. There are two stable conformers, one for each possible chirality. These results are summarized in Figure 3 together with the proposed schematic route for isomer interconversion. In Table 1 we summarize the corresponding values for all **P** and **M** structures.

We can now estimate the barrier for isomer interconversion through the differences of heats of formation between the ground and excited states of the structures at reversed angles: **P-1** at 180 degrees and **M-2** at 0 degrees. From Table 1 (see boldface entries) we can obtain these values: 3.63 eV (A→A′) for **P-1** to **M-2**, and 2.96 eV (B→B′) for **M-2** to **P-1**. These values are very close to those experimentally obtained, 3.40 and 2.85 eV.[9]

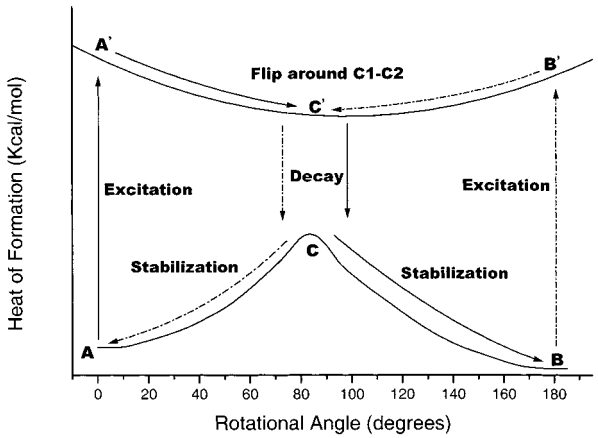

Figure 3. Schematic rotational barrier curves for ground (lower curve) and first excited singlet state (upper curve). The solid and dashed lines indicate the proposed route for isomerization interconversion: **P-1** to **M-2** and **M-2** to **P-1**, respectively. A, B, and C refer to the critical angles at 0, 90, and 180 degrees, respectively.

TABLE 2: Energy, Oscillator Strengths, and Main CI Contributions to the Absorption Threshold (first transition) and the Highest Peak (strongest transition) for the Simulated Absorption Spectra for the Four Structures Shown in Figure 1[a]

molecules	threshold absorption (eV)	oscillator strength (a.u.)	main contributions	maximum absorption (eV)	oscillator strength (a.u.)	main contributions
P-1	2.8679	0.0053	0.9339|H-11→L> + 0.2562|H-11→L+3> + 0.1288|H-11→L+1> − 0.1023|H-12→L>	5.3379	2.6805	0.3314|H-4→L+1> + 0.2858|H-2→L+1> + 0.2547|H→L+5> + 0.2320|H-4→L+6> − 0.2212|H→L+4> − 0.2211|H-3→L+2> − 0.1775|H-4→L+3> − 0.1619|H-5→L+1> + 0.1471|H-3→L+1>
M-2	2.8612	0.0058	0.7159|H→L> + 0.4423|H-3→L> + 0.4243|H-1→L> − 0.1359|H→L+3> − 0.1176|H-5→L> − 0.1137|H-4→L> + 0.1069|H-1→L+3>	5.5512	2.2636	0.4129|H→L+ 7> + 0.2783|H →L+8> + 0.2688|H→L+ 3> − 0.2565|H-4→L+1> − 0.2227|H-2→L+2> + 0.22058|H-4→L> − 0.1835|H-3→L+1> + 0.1676|H-4→L+2> − 0.1028|H-6→L+2>
P-3	2.9192	0.0084	0.8609|H-9→L> + 0.2880|H-9→L+6> − 0.2596|H-10→L> − 01716|H-9→L+3> + 0.1307|H-12→L+12> −0.1019|H-9→L+1>	5.3342	2.8995	0.4444|H-1→L+4> + 0.3172|H-2→L+4> − 0.3050|H →L+7> − 0.2654|H-1→L+3> + 0.2304|H →L+6> − 0.2082|H→L+8> + 0.1984|H+3→L+2> − 0.1975|H-2→L+2> − 0.1716|H-4→L+3> − 0.1407|H-4→L> − 0.1370|H-3→L+1>
M-4	2.9277	0.0031	0.6752|H→L+1> − 0.5069|H→L+2> + 0.3028|H→L+3> − 0.2004|H→L+9> + 0.1964|H→L+5> + 0.1420|H→L+4>	4.8777	3.1952	0.5181|H →L+4> + 0.3763|H-1→L+3> − 0.3337|H-4→L > + 0.2863|H→L+8> + 0.2328|H-2→L+4> + 0.1931|H-1→L+4> − 0.1780|H-1→L+5> + 0.1671|H→L+10> + 0.1669|H-2→L+2> − 0.1446|H-1→L+2> − 0.1332|H-2→L+3> + 0.1033|H-5→L>

(|A→B>) means the configuration generated by taking one electron from A to B level, and H and L refer to HOMO and LUMO, respectively.

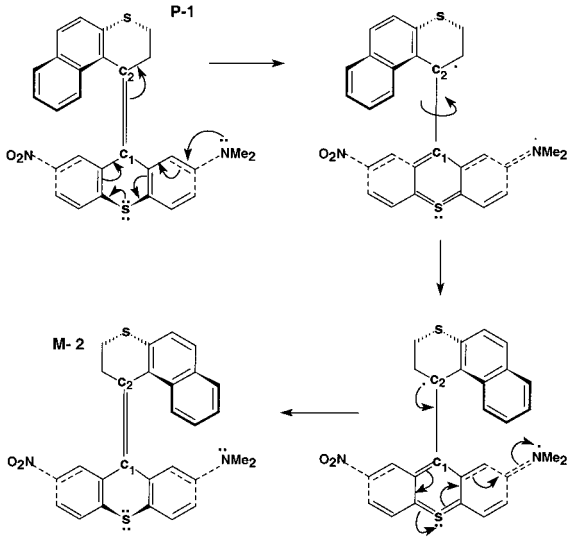

Figure 4. Proposed route for charge transfer and conformational changes for the interconversion **P-1** to **M-2** following appropriate photoexcitation.

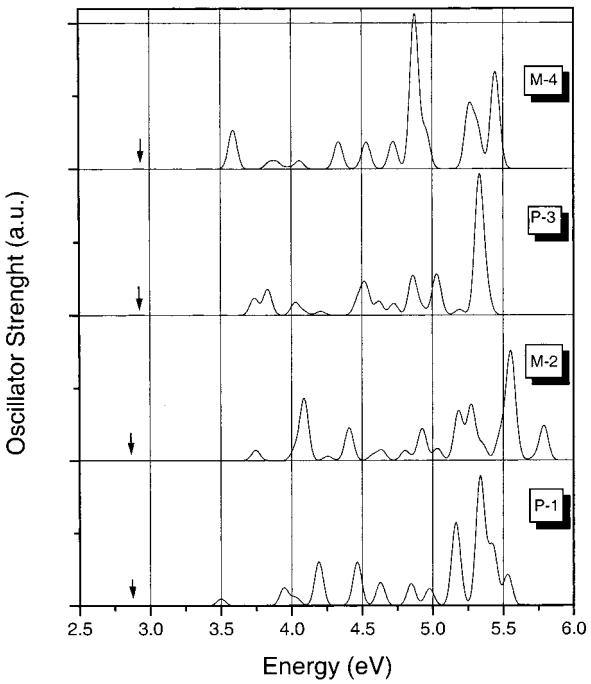

Figure 5. Simulated absorption spectra (in arbitrary units) from ZINDO/S-CI calculations for the four structures shown in Figure 1. The arrows indicate the energy position of the threshold absorptions.

This good agreement shows that this simple approach can effectively provide a reliable estimate for the complex problem of interconversion barriers.

These results also allow us to understand why the protonation blocks the switching process, as schematically indicated in Figure 4. The ground state of **P** and **M** structures contain a double bond (C_1-C_2), and the rotation barriers about double bonds are significantly high (barrier height of ∼1.7 eV, as indicated in Table 1). When **P-1** and **M-2** are photonically excited, one electron is released from the dimethylamino donor group. This produces an elongation of the C_1-C_2 bond and a significant energy stabilization (A′ to C′ or B′ to C′ energy difference values, Figure 3 and Table 1). This effectively removes the rotation barrier around the C_1-C_2 bond, thus allowing flipping and consequently the isomer interconversion (Figure 4). When these structures are protonated, this does not occur (the intramolecular electron transfer is blocked) and the C_1-C_2 bond keeps its double bond character with significantly lower energy stabilization (SE, Table 1). This implies that the barrier remains high, preventing the flipping and consequently the photoisomerization process.

In Table 2 we present a summary from the ZINDO/S-CI calculations for the four structures shown in Figure 1. In Figure 5 we show the corresponding simulated absorption spectra. There is an excellent agreement between the theoretical and the available experimental data on the absorption spectra. The experimental values for the maximum absorption peaks for **P-1** and **M-2** are 5.51 and 5.61 eV,[9] respectively. The corresponding theoretical values are 5.34 and 5.55 eV. For **P-1**, the threshold absorption transition involves molecular states deep in energy, while for **M-2** the frontier molecular orbitals dominate the transitions. For the maximum absorption peaks, the electronic transitions involve typically the last four occupied molecular

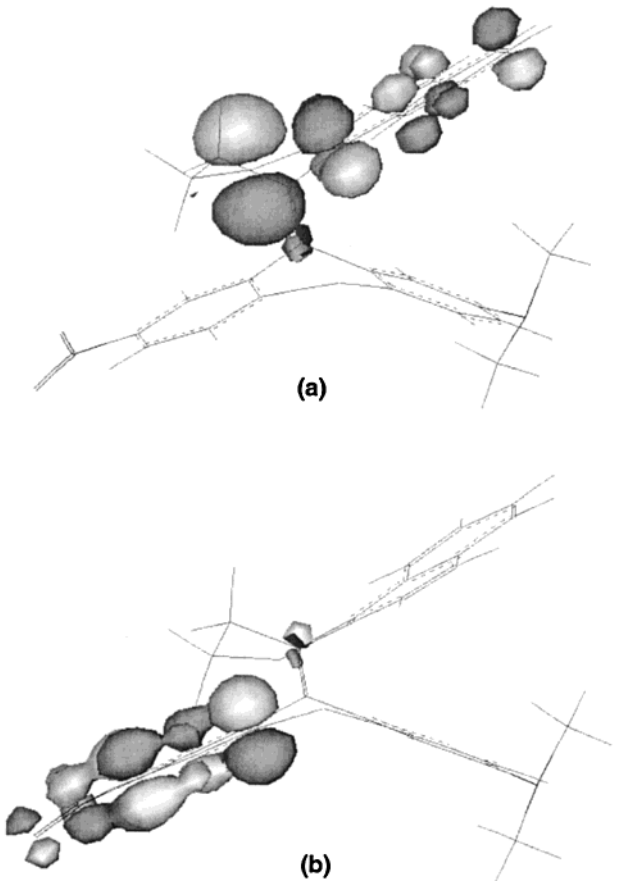

Figure 6. PM3 isosurfaces for **M-2**: (a) HOMO and (b) LUMO.

orbitals and the first four unoccupied ones. The main CI contributions (Table 2) for the threshold absorption tend to present dominant configurations, whereas for the maximum absorption many configurations with similar weight composition are present. This is observed for all four structures.

There are no experimental spectroscopic data available for **P-3** and **M-4** structures. Our results show that there is a small blue shift for the electronic transition threshold values (Table 2, and Figure 5) when we compare **P-1** and **M-2** to **P-3** and **M-4**. On the other hand, a significant red shift for the maximum absorption values is observed only for **M-4**.

The present methodology can in principle be used to analyze and design new and better optical switches. It allows good estimates for the isomer interconversion barriers and very reliable absorption spectra. From the determination of the dominant molecular orbitals of the electronic transitions we have the information of the relative importance of molecular spatial regions participating in the process. For instance, for **M-2** the dominant contribution for the threshold absorption involves the HOMO (highest occupied molecular orbital) and LUMO (lowest unoccupied molecular orbital) levels (Table 2). The isosurface analysis of these orbitals (Figure 6) allows a direct identification of the relevant spatial molecular regions. This information can be very useful for the design of new structures. From appropriate chemical substitution it is possible "to modulate" the desired energy range for optical absorption. This approach could be an effective alternative tool to help researches decrease time and resources devoted to experimental synthesis and testing. Further works along these lines are in progress.

Acknowledgment. This work has been supported in part by the Brazilian Agencies CNPq, FINEP, FAPESP, FAPEMIG, and PREVI/UFJF. We are indebted to the late Prof. M. C. Zerner for kindly making available to us the ZINDO code. The authors thank A. L. L. Garcia for helpful discussions.

Supporting Information Available: A figure showing the P-1 structure and results for the most relevant bond-lengths, bond-angles and dihedrals.

References and Notes

(1) Drexler, K. E. *Nanosystems: Molecular Machinery, Manufacturing and Computation*; Wiley: New York, 1992.
(2) Tsivgoulis, G. M.; Lehn, J.-M. *Chem. Eur. J.* **1996**, *2*, 1399.
(3) Stelacci, F.; Bertarelli, C.; Toscano, F.; Galazzi, M. C.; Zerbi, G. *Chem. Phys. Lett.* **1999**, *302*, 563.
(4) Zijlstra, R. W. J.; Jager, W. F.; de Lange, B.; van Duijnen, P. Th.; Feringa, B. L.; Goto, H.; Saito, A.; Koumura, N.; Harada, N. *J. Org. Chem.* **1999**, *64*, 1667.
(5) Schoevaars, A. M.; Kruizinga, W.; Zijlstra, R. W. J.; Veldman, N.; Spek, A. L.; Feringa, B. L. *J. Org. Chem.* **1997**, *62*, 4943.
(6) Feringa, B. L.; Huck, N. P. M.; Scoevaars, A. M. *Adv. Mater.* **1996**, *8*, 681.
(7) Huck, N. P. M.; Jager, W. F.; de Lange, B.; Feringa, B. L. *Science*, **1996**, *273*, 1686. Huck, N. P. M.; Jager, W. F.; de Lange, B.; Feringa, B. L. *Science*, **1997**, *276*, 341.
(8) Jager, W. F.; de Jong, J. C.; de Lange, B.; Huck, N. P. M.; Meetsma, A.; Feringa, B. L. *Angew. Chem., Int. Ed. Engl.* **1995**, *34*, 348.
(9) Huck, N. P. M.; Feringa, B. L. *J. Chem. Soc., Chem. Commun.* **1995**, 1095.
(10) Feringa, B. L.; Jager, J. F.; de Lange, B. *Tetrahedron* **1995**, *49*, 275.
(11) Barone, P. M. V. B.; Dantas, S. O.; Galvão, D. S. *Synth. Met.* **1999**, *102*, 1454.
(12) Dantas, S. O.; Barone, P. M. V. B.; Braga, S. F.; Galvão, D.S. *Synth. Met.* **2001**, *116*, 275.
(13) Dewar, M. J. S.; McKee, M. L. *J. Am. Chem. Soc.* **1977**, *99*, 5231.
(14) Dewar, M. J. S.; Zoebisch, E. G.; Healy, E. F.; Stewart, J. J. P. *J. Am. Chem. Soc.* **1985**, *107*, 3902.
(15) Stewart, J. J. P. *J. Comput. Chem.* **1991**, *10*, 209 and 221. MOPAC Program, version 6.0 Quantum Chemistry Program Exchange No. 455.
(16) Zerner, M. C. In *Reviews in Computational Chemistry II*, Lipkowitz, K. B., Boyd, D. B. Editors; VCH Publishers: New York, 1991; Chapter 8.
(17) Scano, P.; Thompson, C. *J. Comput. Chem.* **1991**, *12*, 172.
(18) Soos, Z. G.; Galvão, D. S. *J. Phys. Chem.* **1994**, *98*, 1029 and references therein.
(19) Galvão, D. S.; Soos, Z. G.; Ramasesha, S.; Etemad, S. *J. Chem. Phys.* **1993**, *98*, 3016.
(20) Barone, P. M. V. B.; Dantas, S. O.; Galvão, D. S. *J. Mol. Struct. (THEOCHEM)* **1999**, *465*, 219.
(21) Ridley, J.; Zerner, M. C. *Theor. Chim. Acta* **1976**, *42*, 223.
(22) Edwards, W. D.; Zerner, M. C. *Theor. Chim. Acta* **1987**, *72*, 347.
(23) Bolívar-Marinez, L. E.; dos Santos, M. C.; Galvão, D. S. *J. Phys. Chem.* **1996**, *100*, 11029.
(24) Bolívar-Marinez, L. E.; Galvão, D. S.; Caldas, M. J. *J. Phys. Chem. B* **1999**, *103*, 2993.
(25) Spartan Version 4.0, Wavefunction, Inc., 1840 Von Karman Ave., #370 Irvine, CA 92715.
(26) Chem2Pac: A Computational Chemistry Integrator for Windows, M. Cyrillo and D. S. Galvão, http://www.ifi.unicamp.br/gsonm/chem2pac.
(27) Cyrillo, M.; Galvão, D. S. *Eur. Photochem. Assoc. Newsletter* **1999**, *67*, 31.